

TRIGONOMETRIC CURVE-BASED HUMAN MODELING

L. H. You¹, X. S. Yang¹, X. Y. You² and Jian J. Zhang¹
¹*National Centre for Computer Animation, Bournemouth University, Dorset, U.K.*
²*Faculty of Engineering and Computing, Coventry University, Coventry, U.K.*

Keywords: Human modeling, Cross-section curves, Trigonometric series, Surface creation.

Abstract: In this paper, we present a modeling method to build human models. A human model is divided into different parts. For each part, cross-section curves are created and approximated with trigonometric series. All parts are constructed from these trigonometric curves and assembled together to create the whole human model. Since surface creation of human models is transformed into generation of cross-sectional curves and few design parameters are required to describe these cross-sectional curves, our approach can decrease the data size of geometric modeling greatly and is especially suitable for reconstruction of human models from scanned point clouds.

1 INTRODUCTION

Virtual humans are widely applied in various situations such as computer games, virtual reality and digital films. As pointed out by (Thalmann N.M. and Thalmann D., 2005), in order to create realistic and believable virtual humans, three techniques should be developed. They are realistic appearance modeling, realistic, smooth and flexible motion modeling and realistic high-level behaviour modeling.

Among them, realistic appearance achieved by creation and deformation of human models has attracted a lot of research attention.

In the work of (Beylot et al., 1996), the issues of image data for extraction of 3D shapes, surface reconstruction, topological modeling of different anatomical elements and potential applications of topological data base were addressed. (Scheepers et al., 1997) considered the influence of the musculature on exterior form, developed anatomy-based models of muscles which responds to the changes of the posture of an underlying articulated skeleton, and applied them to the torso and arm of a human figure. Modeling muscles, bones, and generalized tissue as triangle meshes or ellipsoids, treating muscles as deformable discretized cylinders whose shapes change as the joints move, creating skin by voxelizing the underlying components, filtering, and extracting a polygonal isosurface, (Jane and Allen, 1997) proposed an improved, anatomically based approach to modeling and animating animals. (Allen et al., 2002) introduced an

example-based method to capture human body scans, estimate poses and kinematics, reconstruct a complete displaced subdivision surface in each pose and combine the surfaces using k-nearest-neighbors scattered data. Based on anatomy concepts, (Nedel and Thalmann, 1998) presented a method which divides a human representation into three different layers: the rigid body from a real skeleton, the muscle design and deformation, and the skin generation. Still using the anatomic model of deformable human bodies consisting of skeleton, muscles and skin, and presenting muscles by the action lines and the muscle shape, they introduced a mass-spring system with angular springs to physically simulate muscle deformations (Nedel and Thalmann, 2000). Defining the space deformed by the control surface by a distance function around the surface, (Singh and Kokkevis, 2000) proposed a surface-oriented FFD which is more suitable for the automated skinning of characters. Deriving muscle motion and deformation from one or several action lines and deforming each action line by a 1D mass-spring system, (Aubel and Thalmann, 2001) proposed a muscle model based on physiological and anatomical considerations. Using a layered canonical model to represent the animal's skeleton, muscles, and skin, generating feature points to deform the attached mesh skin representation, (Maryann et al., 2002) studied a semi-automatic technique for creating 3D models of creatures. (Mohr and Gleicher, 2003) presented a framework for extending linear blending skinning which can capture detailed skin deformations and developed an

automated method to build efficient and accurate character skins from a set of examples. Using motion capture and video cameras and providing a reconstruction algorithm to solve the problems of occlusion, hole-filling, deformation and noise-removal, (Sand et al., 2003) examined how to acquire deformable human geometry from silhouettes. Taking the objective function to be proximity of transformed vertices to the range data, similarity between neighbouring transformations, and proximity of sparse markers at corresponding locations on the template and target surface, (Allen et al., 2003) presented a new method by solving an optimisation problem and explored its applications in human body modeling. (Hyun et al., 2003) represented each limb as a set of ellipsoids of varying size, approximated these ellipsoids with a swept ellipse, determined the difference between the original and approximated limbs using a displacement map, and proposed a new approach to model and deform a human or virtual character's arms and legs. This work was extended to the modeling and deformation of a whole human body, and anatomical features are realised by a GPU-based collision-detection procedure (Hyun et al., 2005). (Seo and Thalmann, 2004) presented a set of techniques to automatically generate a new human body or modify an existing one by manipulating the parameters provided. Using quasi-static linear deformation model and finite element method to calculate the deformation of chunks which represent the internal structures of a virtual character, (Guo and Wong, 2005) gave an approach to create skin deformations. (Venkataraman et al., 2005) introduced a combination of a kinematic and a variational model to deal with the wrinkling of skin by minimising a functional including energies for stretching, bending and self-intersection. By decomposing the facial meshes into the global shape and 3D skin detail and recomposing the shape and 3D skin, (Lee and Soon, 2006) proposed a method to reproduce the scanned model which allows to simulate the exaggeration of the facial global shape, retain the original skin detail and transfer 3D skin from one to another. Using sweeps following a simplified skeleton, (Lee et al., 2006) proposed a new method to carry out realistic human hand modeling and deformation which can achieve real-time performance. (Yang and Zhang, 2006) presented a new anatomy-based skin deformation method which extracts major muscles automatically, formulates muscle sliding around a joint and sliding around a bone, develops a hybrid skin deformation to combine the strengths of anatomy based and

smooth skinning, and is compatible with the current animation workflow. By using the so-called curve skeletons along with the joint-based skeletons, (Yang et al., 2006) investigated an approach to deal with the inherent non-linear relations between the movement of skeletons and the caused skin shapes.

Motivated by the work of (Hyun et al., 2003, 2005) but without using standard ellipses and displacement map, we will introduce trigonometric series to approximate the cross-section curves of a human body, and present a modeling method with a small data size to build human models in this paper.

2 TRIGONOMETRIC SERIES

In the work of (Hyun et al., 2005), sweep surfaces with an elliptic cross section have been used to approximate human arms, legs, torso and neck, and carry out human modeling and deformation. The mathematical description of sweep surfaces has the form of

$$\begin{aligned} \mathbf{S}(u, v) &= \mathbf{R}(u)\mathbf{E}_u(v) + \mathbf{C}(u) \\ &= \begin{bmatrix} r_{11}(u) & r_{12}(u) & r_{13}(u) \\ r_{21}(u) & r_{22}(u) & r_{23}(u) \\ r_{31}(u) & r_{32}(u) & r_{33}(u) \end{bmatrix} \begin{bmatrix} a(t)\cos(v) \\ b(t)\sin(v) \\ 0 \end{bmatrix} + \begin{bmatrix} x(u) \\ y(u) \\ z(u) \end{bmatrix} \end{aligned} \quad (1)$$

where $\mathbf{S}(u, v)$ is a sweep surface, $\mathbf{R}(u)$ and $\mathbf{C}(u)$ stand for rotation and translation, respectively, and $\mathbf{E}_u(v)$ is a standard ellipse of variable size.

Since the cross sections of most parts of a human body are irregular curves. Using standard ellipses to approximate these cross sections will bring in some errors.

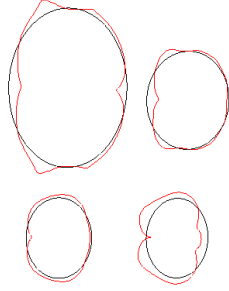
As indicated in Figure 1, we give some cross-section curves of human torso from a human model built with the polygon modeling approach and those approximated by elliptic cross sections where the curves in red indicate cross-section curves and those in blue are from standard ellipses. It can be seen for these images that there are noticeable differences between the real cross-section curves and elliptic ones.

In addition, for a certain value u_0 of the parametric variable u , Eq. (1) can be written as the following form

$$\begin{aligned} S_x(u_0, v) &= f_{11}(u_0)\cos(v) + f_{12}(u_0)\sin(v) + x(u_0) \\ S_y(u_0, v) &= f_{21}(u_0)\cos(v) + f_{22}(u_0)\sin(v) + y(u_0) \\ S_z(u_0, v) &= f_{31}(u_0)\cos(v) + f_{32}(u_0)\sin(v) + z(u_0) \end{aligned} \quad (2)$$

The above equation indicates that at the plane determined by a point $\mathbf{C}(u_0)$ and a unit normal vector $\mathbf{N}(u_0) = [r_{13}(u_0) \ r_{23}(u_0) \ r_{33}(u_0)]^T$, the cross-

section curve of the sweep surface is a simple curve which is described with two trigonometric functions $\cos(v)$ and $\sin(v)$.



Cross-section curves of torso

Figure 1: Comparison between real human cross-section curves and approximated ellipses.

In order to describe the cross-section curves of a human body more accurately, we propose to use trigonometric series to represent cross-section curves. With the application of more terms of trigonometric series, the cross-section curves of a human body can be approximated very accurately.

In the previous work (You et al., 2004), trigonometric series has been applied to describe blending surfaces. By degenerating the two dimensional problems to one dimensional ones, the trigonometric series proposed by (You et al., 2004) can be modified to represent cross-section curves of a human body. Assuming that a cross-section curve is perpendicular to one of x - y , x - z and y - z plane, with the centre $C = [x_c \ y_c \ z_c]^T$, and taking the one perpendicular to x - y plane as an example, the mathematical equation of the cross-section curve can be written in the following trigonometric series

$$\begin{aligned} x - x_c &= a_0 + \sum_{j=1}^J (a_{2j-1} \cos jv + a_{2j} \sin jv) \\ y - y_c &= b_0 + \sum_{j=1}^J (b_{2j-1} \sin jv + b_{2j} \cos jv) \\ z - z_c &= 0 \end{aligned} \quad (3)$$

where a_j and b_j ($j=0,1,2,3,\dots,2J$) are unknown constants.

If there is a cross-section curve represented by a number of discrete points (x_i, y_i, z_c) ($i=1,2,3,\dots,I$), the centre of the cross-section curve can be determined by the average value of each component x and y . That is

$$\begin{aligned} x_c &= \frac{1}{I} \sum_{i=1}^I x_i \\ y_c &= \frac{1}{I} \sum_{i=1}^I y_i \end{aligned} \quad (4)$$

Then, we use curve fitting and the least squares algorithm to determine the unknown constants in Eq. (3). To this aim, we calculate the squares sum of the errors between the curve and the trigonometric series at the points (x_i, y_i, z_c) ($i=1,2,3,\dots,I$) for x and y position components, respectively

$$\begin{aligned} E_x &= \sum_{i=1}^I [x_i - x_c - a_0 \\ &\quad - \sum_{j=1}^J (a_{2j-1} \cos jv_i + a_{2j} \sin jv_i)]^2 \\ E_y &= \sum_{i=1}^I [y_i - y_c - b_0 \\ &\quad - \sum_{j=1}^J (b_{2j-1} \sin jv_i + b_{2j} \cos jv_i)]^2 \end{aligned} \quad (5)$$

The errors in Eq. (5) are minimized by setting the derivatives of the square sums with respect to the unknown constants to zero

$$\begin{aligned} \frac{\partial E_x}{\partial a_j} &= 0 \\ \frac{\partial E_y}{\partial b_j} &= 0 \\ (j &= 0,1,2,3,\dots,2J) \end{aligned} \quad (6)$$

which leads to the following linear algebraic equations

$$\begin{aligned} \sum_{i=1}^I (x_i - x_c) - \sum_{i=1}^I a_0 - \sum_{j=l=1}^J \sum_{i=1}^I a_{2j-1} \cos jv_i - \sum_{j=l=1}^J \sum_{i=1}^I a_{2j} \sin jv_i &= 0 \\ \sum_{i=1}^I (x_i - x_c) \cos kv_i - a_0 \sum_{i=1}^I \cos kv_i - \sum_{j=l=1}^J \sum_{i=1}^I a_{2j-1} \cos jv_i \cos kv_i - \sum_{j=l=1}^J \sum_{i=1}^I a_{2j} \sin jv_i \cos kv_i &= 0 \\ \sum_{i=1}^I (x_i - x_c) \sin kv_i - a_0 \sum_{i=1}^I \sin kv_i - \sum_{j=l=1}^J \sum_{i=1}^I a_{2j-1} \cos jv_i \sin kv_i - \sum_{j=l=1}^J \sum_{i=1}^I a_{2j} \sin jv_i \sin kv_i &= 0 \\ (k &= 1,2,3,\dots,J) \end{aligned} \quad (7)$$

and

$$\begin{aligned} \sum_{i=1}^I (y_i - y_c) - \sum_{i=1}^I b_0 - \sum_{j=l=1}^J \sum_{i=1}^I b_{2j-1} \sin jv_i - \sum_{j=l=1}^J \sum_{i=1}^I b_{2j} \cos jv_i &= 0 \\ \sum_{i=1}^I (y_i - y_c) \sin kv_i - b_0 \sum_{i=1}^I \sin kv_i - \sum_{j=l=1}^J \sum_{i=1}^I b_{2j-1} \sin jv_i \sin kv_i - \sum_{j=l=1}^J \sum_{i=1}^I b_{2j} \cos jv_i \sin kv_i &= 0 \\ \sum_{i=1}^I (y_i - y_c) \cos kv_i - b_0 \sum_{i=1}^I \cos kv_i - \sum_{j=l=1}^J \sum_{i=1}^I b_{2j-1} \sin jv_i \cos kv_i - \sum_{j=l=1}^J \sum_{i=1}^I b_{2j} \cos jv_i \cos kv_i &= 0 \\ (k &= 1,2,3,\dots,J) \end{aligned} \quad (8)$$

Solving equations (7) and (8), respectively, we determine all unknown constants and obtain the mathematical representation of the cross-section curve.

For the curve which is not perpendicular to any coordinate planes, we must carry out the coordinate transformation and find the mathematical description of the curve in the local coordinate system where one of the coordinate axes is perpendicular to the plane containing the curve.

For some representative curves taken from human leg and torso, we use the trigonometric series (3) and standard ellipse $E_u(v)$ to regenerate them and the obtained results were depicted in Figure 2 where J is defined in Eq. (3), the curve in red is the original one, the one in green is from the algorithm of the trigonometric series, and that in blue is created with the equation of the standard ellipse.

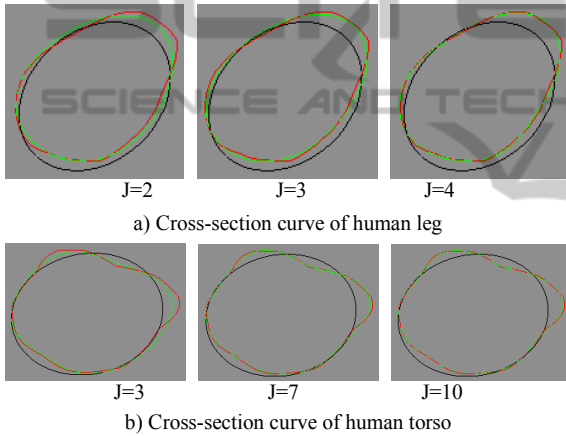


Figure 2: Curve generation with different approaches.

It can be seen from these curves that the algorithm of the trigonometric series can approximate the cross-section curves of human body quite well and the approximation can be greatly improved by increasing the terms of the trigonometric series. Since most cross-section curves of a human body have the similar complexity to those in this figure, the proposed approach can use few terms to achieve high accuracy of curve modeling.

Depending on different shapes of cross-section curves, different terms in Eq. (3) will be used to achieve the required accuracy. Too few terms in Eq. (3) will cause too large errors. Too many terms will increase the computational cost and slow down the human modeling process. Therefore, suitable terms should be used. In the situation of interactive modeling, it is required to automatically find out which value of the term J is the best. In order to

tackle this issue, here we propose the following strategy.

First, we define an average error E_a and a maximum error E_M below. The former is used to measure the global approximation of the curve from the trigonometric series to the original curve and the latter quantifies the maximum difference between the curve from the trigonometric series and the original curve.

$$E_a = \frac{1}{I} \sum_{i=1}^I \frac{d_i}{d_i} \quad (9)$$

and

$$E_M = \max \left\{ \frac{d_1}{d_1}, \frac{d_2}{d_2}, \frac{d_3}{d_3}, \dots, \frac{d_J}{d_J} \right\} \quad (10)$$

where

$$\begin{aligned} d_i &= \sqrt{d_{xi}^2 + d_{yi}^2} \\ \bar{d}_i &= \sqrt{(x_i - x_c)^2 + (y_i - y_c)^2} \\ d_{xi} &= x_i - x_c - a_0 - \sum_{j=1}^J (a_{2j-1} \cos jv_i + a_{2j} \sin jv_i) \\ d_{yi} &= y_i - y_c - b_0 - \sum_{j=1}^J (b_{2j-1} \sin jv_i + b_{2j} \cos jv_i) \end{aligned} \quad (11)$$

Then, we set different errors to determine the required terms in Eq. (3). For example, we take the average error and maximum error not more than 1% and 5%, respectively. That is

$$\begin{aligned} E_a &\leq 1\% \\ E_M &\leq 5\% \end{aligned} \quad (12)$$

A linear interpolation operation is employed to find out the suitable terms efficiently. Initially, we take $J=3$ and $J=10$, and calculate the average errors E_{a3} and E_{a10} and the maximum errors E_{m3} and E_{m10} where the subscripts 3 and 10 stand for the values of J . If both E_{a3} and E_{m3} have met Eq. (12), or one of E_{a10} and E_{m10} does not satisfy Eq. (12), a linear extrapolation operation is used to find a smaller J_1 for the former and a larger J_1 for the latter. Otherwise, a linear interpolation is applied to calculate the J_1 between $J=3$ and $J=10$. The obtained J_1 is usually not an integer. We round off it to the nearest integer. With J_1 , we calculate the average errors E_{aJ_1} and the maximum errors E_{mJ_1} and examine whether they have met Eq. (12). If both E_{aJ_1} and E_{mJ_1} have met Eq. (12) and $J_1 < 3$, the linear extrapolation operation occurs with J_1 and

$J=3$. If one of E_{aJ_1} and E_{mJ_1} does not satisfy Eq. (12) and $J_1 > 10$, the linear extrapolation operation is performed with $J=10$ and J_1 . If both E_{aJ_1} and E_{mJ_1} have met Eq. (12) and $3 < J_1 < 10$, the linear interpolation operation is conducted between $J=3$ and J_1 . If one of E_{aJ_1} and E_{mJ_1} does not satisfy Eq. (12) and $3 < J_1 < 10$, the linear interpolation operation is carried out between J_1 and $J=10$.

Since there are two quantities E_a and E_m which can be employed for the interpolation, we must determine which one should be used. Obviously, if only one of E_a and E_m does not meet Eq. (12), this error is used for the interpolation. If both of them do not satisfy Eq. (12), we always use the average error for the interpolation since the average error is a global measurement of the difference between the original curve and that from the trigonometric series.

3 HUMAN PARTS DEFINED WITH TRIGONOMETRIC SERIES

In order to build a human model, we draw some cross-section curves which define the human profiles. Then we approximate the original cross sections with the trigonometric series. After that, we construct surface patches from the curves generated using the trigonometric series with the following treatment.

As mentioned by (Tokuyama, 2000), among three surface interpolation methods, i. e., interpolating through distinct point data, skinning over a family of curves and interpolating the surface simultaneously over two families of intersection curves, the skinning method is generally considered to be the most frequently used technique for surface construction. Here we use this skinning method to construct surface patches of human parts.

If a surface patch will be constructed from K curves determined with the trigonometric series $(c_{xk}(v), c_{yk}(v), c_{zk}(v))$ ($k=0, 1, 2, 3, \dots, K-1$) where $c_{xk}(v)$, $c_{yk}(v)$ and $c_{zk}(v)$ are determined by Eq. (3), we use the following equation to describe the surface to be constructed

$$t(u, v) = \sum_{m=0}^{K-1} u^m f_{im}(v) \quad (13)$$

$(t = x, y, z)$

where $f_{im}(v)$ ($m=0, 1, 2, 3, \dots, K-1$) are unknown functions.

Uniformly dividing the region $u=0$ to $u=1$ into $K-1$ equal intervals which gives the interval length to be $du=1/(K-1)$, we have $u_k = k \times du$ ($k=0, 1, 2, 3, \dots, K-1$). The unknown functions $f_{im}(v)$ ($m=0, 1, 2, 3, \dots, K-1$) can be determined by solving the following linear algebraic equations

$$c_{tk}(v) = \sum_{m=0}^{K-1} u_k^m f_{im}(v) \quad (14)$$

$(k = 0, 1, 2, 3, \dots, K-1; t = x, y, z)$

Expanding Eq. (14) and rewriting it into the form of matrix, we obtain the following mathematical expression

$$[R_t(u_{km})]\{F_t(v)\} = \{C_t(v)\} \quad (15)$$

where $[R_t(u_{km})]$ is a $K \times K$ square matrix with the elements $u_{km} = u_k^m$ ($k=0, 1, 2, \dots, K-1; m=0, 1, 2, \dots, K-1$), $\{F_t(v)\} = [f_{t0}(v) \ f_{t1}(v) \ f_{t2}(v) \ \dots \ f_{tK-1}(v)]^T$ and $\{C_t(v)\} = [c_{t0}(v) \ c_{t1}(v) \ c_{t2}(v) \ \dots \ c_{tK-1}(v)]^T$ are two vectors with K elements.

Using $[R_t(u_{km})]^{-1}$ to indicate the inverse matrix of $[R_t(u_{km})]$ and left multiplying both sides of Eq. (15) by this inverse matrix, we obtain the unknown functions with the following equation

$$\{F_t(v)\} = [R_t(u_{km})]^{-1} \{C_t(v)\} \quad (16)$$

At the boundary curves where two different surface patches are to be connected together, we must consider the continuity between the two surface patches. For an existing surface patch indicated by Eq. (13), different order continuities such as the boundary tangents and boundary curvature etc. at its boundaries can be determined from the different orders of partial derivatives

$\frac{\partial t^n(u, v)}{\partial u^n}$ ($n=1, 2, 3, \dots$) of the surface patch with respect to the parametric variable u . By introducing these partial derivatives into the above operation, different order continuities between two connected surface patches can be obtained.

For example, if we intend to connect two surface patches with the tangent continuity at $u=1$ of the existing surface patch $\bar{t}(u, v)$, we obtain the mathematical expressions of the first partial derivative $\left[\frac{\partial \bar{t}(u, v)}{\partial u} \right]_{u=1} = \sum_{m=1}^{K-1} m \bar{f}_{im}(v)$ of the existing

surface patch $\bar{t}(u,v)$ and $\left[\frac{\partial t(u,v)}{\partial u}\right]_{u=0} = f_{t1}(v)$ of the unknown surface patch $t(u,v)$ with respect to the parametric variable u from Eq. (13), respectively. Then the following tangential continuity constraint is added to Eq. (14).

$$f_{t1}(v) = \sum_{m=1}^{K-1} m \bar{f}_{tm}(v) \quad (17)$$

$(t = x, y, z)$

Since one more linear algebraic equation is introduced, the unknown functions $f_{tm}(v)$ in Eq. (13) should be increased from $f_{tK-1}(v)$ to $f_{tK}(v)$ and all K in Eq. (13) and thereafter will be replaced by $(K+1)$.

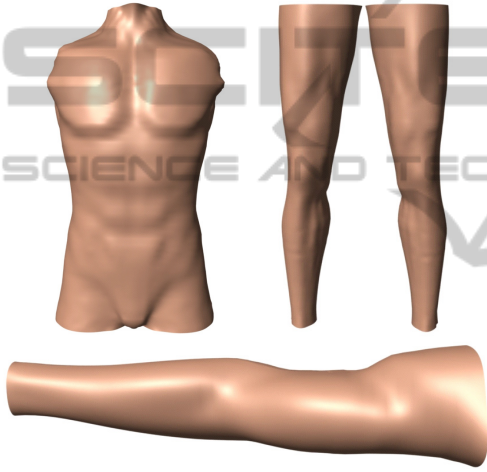


Figure 3: Human torso, legs and arm created from the trigonometric series.

If both opposite edges of a surface patch $t(u,v)$ will be connected to two separate surface patches $\bar{t}(u,v)$ and $\bar{\bar{t}}(u,v)$, the continuity at the boundary curve $u=0$ of the exiting surface patch $\bar{\bar{t}}(u,v)$ should also be considered. Similar to the above treatment, the following boundary condition for the tangential continuity will be added to Eq. (14)

$$\sum_{m=1}^{K-1} m \bar{f}_{tm}(v) = \bar{\bar{f}}_{t1}(v) \quad (18)$$

$(t = x, y, z)$

and the unknown functions $f_{tm}(v)$ in Eq. (13) will be increased to $f_{tK+1}(v)$ and all K in Eq. (13) and thereafter will be replaced by $(K+2)$.

With the above constructed surface function, we create human torso, legs and arms from the trigonometric series as demonstrated in Figure 3.

4 ASSEMBLY OF HUMAN PARTS BY SURFACE BLENDING

After successful construction of human parts including human torso, arms, and legs, the remaining task is how to assemble them together which maintains smooth transition between different human parts and ensures the surface in the transition region has the realistic appearance of the human part.

There are two approaches which can be used to achieve this aim: one is surface blending (Zhang and You, 2004) and the other is local extrusion deformation (You and Zhang, 2003). Here we take the connection between human torso and right arm as an example to explain the operation of surface blending.

Firstly, we determine the boundary curves and boundary tangents of the surface which will smoothly connect human right arm to torso together. According to the position function of the surface patch at the leftmost end of the right arm, we can determine the right boundary curve and boundary tangent of the transition surface. In order to determine the left boundary curve and boundary tangent of the transition surface, we create a cross-sectional curve on the human torso near the left end of the right arm and calculate the tangent of the human torso at this curve. Then, we construct the transition surface with these boundary curves and boundary tangents. We can change the size of the boundary tangents to change the shape of the transition surface and to make the transition surface look more realistically. If the manipulation of the boundary tangents does not reach the required realism, we add one or more cross-section curves between the two boundary curves and create the transition surface from two boundary curves, two boundary tangents and the in-between curves. With such a method, we connect two different parts together. The top image of Figure 4 gives two human parts: right arm and torso, and the bottom image shows these two human parts have been smoothly connected together. With the same treatment, we also connected the left arm to the torso.

For the connection between the human torso and legs, we first use a surface to close the bottom opening of the human torso. Then we determine boundary curves and tangents of the torso corresponding the right and left legs, respectively. And finally, the above method is employed to produce the transition surfaces between the three human parts.

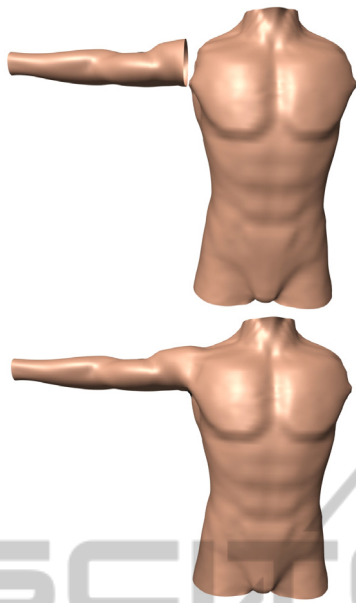


Figure 4: Connection of different human parts.

In Figure 5, we gave a human model built with our proposed approach.

The approach presented in this paper greatly lowers the data size of geometric modeling. For the human body given in the following figure, the modeling with the polygon approach uses 6457 vertices with total 14371 design parameters to create the model. With our method, only 6510 design parameters are required to build it.

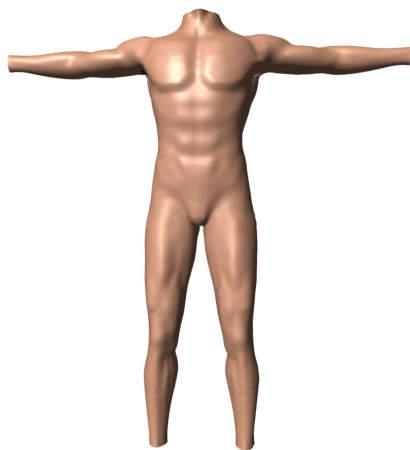


Figure 5: Human model assembled from different human parts.

5 CONCLUSIONS

Human modeling can be performed with NURBS, polygon and subdivision. These approaches are

effective and popular. However, they involve a lot of design parameters. In order to reduce design parameters, we present a new modeling method to build human models.

The method starts from cross-sectional curves of a human body. With introduction of trigonometric series, these cross-sectional curves are approximated very accurately. Then human parts are constructed from the curves generated with the trigonometric series. We examined how to construct human parts from these trigonometric curves and demonstrated that surface patches produced with our proposed approach can maintain the required continuities between two adjacent patches. Finally, we discussed the assembly issue of human models.

Unlike the sweep-based human modeling, our method can represent cross-sectional curves of human body very accurately. Due to this reason, the treatment to improve the modeling realism using some approaches such as displacement map is not required.

Our proposed approach greatly reduces design parameters of human modeling. It is especially suitable for reconstruction of human models from scanned point clouds.

REFERENCES

- Allen, B., Curless, B., Popović, Z., 2002. Articulated body deformation from range scan data. *In Proceedings of the 2002 Conference on Computer Graphics, SIGGRAPH*, ACM Press, 173-180.
- Allen, B., Curless, B., Popović, Z., 2003. The space of human body shapes: reconstruction and parameterization from range scans. *ACM Transactions on Graphics* 22(3), 587-594.
- Aubel, A., Thalmann, D., 2001. Interactive modeling of the human musculature. *In Proceedings of Computer Animation*, Institute of Electrical and Electronics Engineers Inc., 167-173.
- Beylot, P., Gingsins, P., Kalra, P., Thalmann, N. M., Maurel, W., Thalmann, D., Fasel, J., 1996. 3D interactive topological modeling using visible human dataset. *EUROGRAPHICS '96 and Computer Graphics Forum* 15(3), 33-44.
- Guo, Z., Wong, K. C., 2005. Skinning with deformable chunks. *EUROGRAPHICS 2005 and Computer Graphics Forum* 24(3), 373-381.
- Hyun, D.-E., Yoon, S.-H., Kim, M.-S., Jüttler, B., 2003. Modeling and deformation of arms and legs based on ellipsoidal sweeping. *In Proceedings of 11th Pacific Conference on Computer Graphics and Applications*, IEEE Computer Society, 204-212.
- Hyun, D.-E., Yoon, S.-H., Chang, J.-W., Kim, M.-S., Jüttler, B., 2005. Sweep-based human deformation. *The Visual Computer* 21, 542-550.

- Jane, W., Allen, V. G., 1997. Anatomically based modeling, *In Proceedings of the 1997 Conference on Computer Graphics*, SIGGRAPH, ACM Press, 173-180.
- Lee, W.-S., Soon, A., 2006. Facial shape and 3D skin. *Computer Animation and Virtual Worlds 17*, 501-512.
- Lee, J., Yoon, S.-H., Kim, M.-S., 2006. Realistic human hand deformation. *Computer Animation and Virtual Worlds 17*, 479-489.
- Maryann, S., Jane, W., Allen, V. G., 2002. Model-based reconstruction for creature animation. *In Conference Proceedings on ASM SIGGRAPH Symposium on Computer Animation*, Institute of Electrical and Electronics Engineers Inc., 139-146.
- Mohr, A., Gleicher, M., 2003. Building efficient, accurate character skins from examples. *ACM Transactions on Graphics 22(3)*, 562-568.
- Nedel, L., Thalmann, D., 1998. Modeling and deformation of human body using an anatomically-based approach. *In Proceedings of the Computer Animation*. IEEE Computer Society, 34-40.
- Nedel, L., Thalmann, D., 2000. Anatomic modeling of deformable human bodies. *The Visual Computer 16*, 306-321.
- Sand, P., McMillan, L., Popović, J., 2003. Continuous capture of skin deformation. *SIGGRAPH 2003 and ACM Transactions on Graphics 22(3)*, 578-586.
- Scheepers, F., Parent, R. E., Carlson, W. E., May, S. F., 1997. Anatomy-based modeling of the human musculature. *In Proceedings of the 24th Annual Conference Computer Graphics and Interactive Techniques*, ACM Press/Addison-Wesley Publishing Co., 163-172.
- Seo, H., Thalmann, N. M., 2004. An example-based approach to human body manipulation. *Graphical Models 66*, 1-23.
- Singh, K., Kokkevis, E., 2000. Skinning character using surface-oriented free-form deformations. *In Proceedings of Graphics Interface, 2000*. Canadian Information Processing Soc., 35-42.
- Thalmann, N. M., Thalmann, D., 2005. Virtual humans: thirty years of research, what next? *The Visual Computer 21*, 997-1015.
- Tokuyama, Y., 2000. Skinning-surface generation based on spine-curve control. *The Visual Computer 16*, 134-140.
- Venkataraman, K., Lodha, S., Raghavan, R., 2005. A kinematic-variational model for animating skin with wrinkles. *Computers & Graphics 29*, 756-770.
- Yang, X. S., Zhang, J. J., 2006. Automatic muscle generation for character skin deformation. *Computer Animation and Virtual Worlds 17*, 293-303.
- Yang, X. S., Somasekharan, A., Zhang, J. J., 2006. Curve skeleton skinning for human and creature characters. *Computer Animation and Virtual Worlds 17*, 281-292.
- You, L. H., Zhang, J. J. 2003. Fast generation of 3-D deformable surfaces. *IEEE Transactions on Systems Man and Cybernetics: Part B-Cybernetics 33(4)*, 616-625.
- You, L. H., Comminos, P., Zhang, J. J., 2004. PDE blending surfaces with C^2 continuity. *Computers and Graphics 28(6)*, 895-905.
- Zhang, J. J., You, L. H., 2004. Fast surface modeling using a 6th order PDE. *Computer Graphics Forum 23(3)*, 311-320.